RSC Advances

ROYAL SOCIETY OF CHEMISTRY

www.rsc.org/advances

RSC Advances

PAPER

Electrospinning-derived ultrafine silver-carbon composite nanofibers for flexible transparent conductive films

Received 00th January 20xx,
Accepted 00th January 20xx

DOI: 10.1039/x0xx00000x
www.rsc.org/

Liwen Zhang[a], Yejun Qiu[a,*], Hong Liu[b]

Abstract: Ultrafine silver/carbon composite nanofibers (Ag/CNFs) were prepared by electrospinning. Silver nanoparticles uniformly distributed in the fibers and enhanced their conductivity to some degree. The Ag/CNFs partially substituting silver nanowires (AgNWs) to fabricate transparent conductive films (TCFs) were investigated. The order of depositing Ag/CNFs and AgNWs would exert great effect on the property of the TCFs, and first deposition of AgNWs followed by Ag/CNFs was preferred. With the increase of the density of the deposited Ag/CNFs, the sheet resistance of the TCFs firstly decreased obviously and then increased slightly after reaching a minimum value. When decreasing the fiber diameter, the transparency increased dramatically, while the conductivity changed slightly. The TCFs fabricated using the Ag/CNFs with a fiber diameter of about 30 nm and a substitution value of 41.7% had a sheet resistance of 124.5 Ω/sq and transparency of 88.0%, while a sheet resistance of 83.0 Ω/sq and transparency of 87.5% could be achieved if lowering substitution amount to 28.3%; and after experiencing proper heat treatment and acid immersion, the conductivity can be further improved to 50.0 Ω/sq. Additionally, it was found that the as-prepared hybrid TCFs exhibited good flexibility, strong adhesion, and good resistance to high temperature as well as strong acid conditions.

1. INTRODUCTION

With advances in displays, touch panels, and solar cells, there is an ever increasing demand for low-cost transparent electrode materials, and currently indium tin oxide (ITO) is most widely used. Although ITO has been applied for several decades, the limited supply of indium restricts its future applications. In addition, the ITO film is unsuitable for flexible displays and electronics because it tends to produce a brittle fracture after even 1% strain.[1,2] Therefore, there is an urge demand for novel materials to replace ITO in the application of transparent conductive films (TCFs). There are several candidates for substituting ITO, mainly including conducting polymers,[3-5] carbon nanotubes,[6-8] graphene,[9-11] ultra-thin metal films,[12] metal grids,[13,14] metal nanowires,[15-17]and theirhybrids.[18-20] Among these contenders, random silver nanowire (AgNW) networks show excellent optoelectronic performance very close to that of ITO.[21] However, the contact resistance induced by the polymer remained on the surface of AgNWs is still high[22] and the resistance towards harsh environments is poor due to high activity of AgNWs[23,24].Besides, the fabrication of AgNWs is expensive and accompanied with large solvent emission, and the difficulty of further increasing the ratio of length to diameter (L/D) offers another challenge[25].

Recently, many efforts have been made to reduce inter-nanowire contact resistance and replace AgNWs thoroughly or partially by adopting cheaper and more weatherable materials. On one hand, the contact resistance is reduced by increasing the contact area between AgNWs through light-induced plasmonic welding technique[26], heat treatment[27], and mechanically pressing[28]. On the other hand, fabricating composite film with combination of AgNWs and other conductive interconnecting materials such as graphene[29, 30] and carbon nanotubes[31] has been proved effective to provide protections and cut down the costs. However, the former route could still not solve the relatively high cost and poor resistance to environment of AgNWs, while the developed interconnecting materials in the later possess low ratio of L/D and are difficult to weld with AgNWs. Therefore, it is highly desired to develop methods to synthesize novel materials with cheap cost, high stability, large L/D value, and easiness to decrease contact resistance.

As is known, electrospinning is a simple, versatile and effective method to produce continuous one-dimensional nanomaterials with large ratio of L/D. Therefore, this method is considered to fabricate a novel conductive material of silver/carbon composite nanofibers (Ag/CNFs). Carbon element is stable in many rigorous environments and probably suitable to substitute AgNWs once it develops into fiber morphology. Additionally, the introduction of silver is

[a] Shenzhen Engineering Lab of Flexible Transparent Conductive Films, Department of Materials Science and Engineering, Shenzhen Graduate School, Harbin Institute of Technology, University Town, Shenzhen, 518055, China. E-mail: yejunqiu@hitsz.edu.cn.; Tel:+86-755-26032462; Fax: +86-755-26033504.
[b] School of Materials Science and Engineering, South China University of Technology, Guangzhou, 510640, China
Electronic Supplementary Information (ESI) available. SeeDOI: 10.1039/x0xx00000x

beneficial to improve the fiber conductivity as well as decrease the contact resistance greatly due to the fusion of Ag nanoparticles in the fibers with AgNWs. Thus, Ag/CNFs are promising materials to thoroughly or partially substitute AgNWs in fabricating TCFs. To best of our knowledge, there are no reports on the TCFs fabricated with Ag/CNFs.

In this work, by using electrospinning-derived ultrafine and ultra-long Ag/CNFs as novel conductive material, hybrid TCFs were fabricated. The comprehensive performance of Ag/CNFs to replace AgNWs was well probed into. Interestingly, the resultant hybrid TCFs produced by ultrafine Ag/CNFs and AgNWs exhibit high transmittance, good conductance, and excellent resistance to harsh environments.

2. EXPERIMENTAL SECTION

2.1 Chemicals and materials.

Poly-acrylonitrile (PAN, Mw=150,000), silver nitrate ($AgNO_3$), glucose, acetone, N,N-Dimethylformamide (DMF), hydrochloric acid (HCl), poly ethylene terephthalate (PET, with average transmittance of 93%) and mixed cellulose ester membranes (MF-Millipore Membrane, USA, mixed cellulose esters, hydrophilic, 0.4 μm. 47 mm) were purchased from commercial suppliers. AgNWs with average length of 20 μm and average diameter of 50 nm (Figure S1a) were purchased from Guangzhou Qianshun Industrial Material Co., Ltd and were supplied as a suspension in isopropyl (IPA). An aliquot of the AgNWs suspension was diluted to 0.1 mg/mL with IPA and stored until use. All chemicals were used without further purification.

2.2 Synthesis and characterization of Ag/CNFs.

The Ag/CNFs were synthesized through electrospinning and subsequent carbonization under NH_3 atmosphere. In a typical procedure of electrospinning, an amount of PAN was dissolved into DMF to form uniform aqueous. Thereafter, $AgNO_3$ and glucose were blended in turn into the mixture. The weight ratio of these three reagents is 2:1:1. After stirring for over 24 hours in a dark room, the solutions with light yellow colour were fed into an ordinary hypodermic syringe with a stainless steel needle which is connected with a high voltage power supply (0–50 kV) (DWP503-2ACCD, Dong wen High Voltage Power Supply Company, China). During electrospinning, the applied voltage, tip-to-collector distance, and flow feed rate are 10 kV, 10 cm, and 2 mL/h, respectively. Finally, the non-woven fiber samples were treated in NH_3 at 1000°C for 30 min. The sample morphology, component, and structure were characterized by scanning electron microscopy/energy dispersive spectroscopy (SEM/EDS, HITACHI S-4700), transmission electron microscopy (TEM, JEM2010), X-ray diffraction (XRD, Rigaku D/Max 2500/PC), and Raman spectroscopy (Renishaw RM-1000) .

2.3 Fabrication and characterization of TCFs.

As shown in Figure S2, the Ag/CNF fibers were firstly dispersed into water with an optimized concentration through persistently ultrasonic treatment, and Figure S1b gives the optical photos. Then the composite films containing AgNWs and Ag/CNFs with surface loadings of 28-53 mg/m^2 and 20-160 mg/m^2, respectively, were prepared via transfer-free vacuum filtration through mixed cellulose ester membranes. Thereafter, the films were adhered on a PET substrate and exposed to acetone vapour for ten minutes at 55°C to reveal its transparent property, and finally the TCF samples were obtained. The optical transmittance were measured by a UV-vis spectrometer at wavelengths ranging from 380 to 800 nm (SHIMADZU, UV-3600), and the sheet resistance was measured using a four point probe (KEITHLEY 6221/2182A). The average transmittance values at a wavelength of 550 nm was used as the optical transmittance of TCFs, and the reported sheet resistance values were also an average of ten measurements on two separate samples. The resistance to thermal oxidation was tested by treating the TCFs at different temperatures ranging from 90°C to 170°C. And the resistance to acid corrosion was tested through immersing the TCFs into hydrochloric (HCl) acid solution with different concentration. Moreover, the structure of the TCFs was also observed by SEM.

3. RESULTS AND DISCUSSION

The Ag/CNFs composite nanofibers were produced by electrospinning mixture solutions containing PAN, $AgNO_3$ and glucose, and subsequent carbonization of the as-spun fiber precursors in NH_3 at high temperature. During the fabrication process, the addition of glucose and direct carbonization without pre-oxidation treatment are beneficial to maintain fibrous morphology, and the structure of silver embedded inside carbon can be gotten by adopting suitable flow rate of NH_3 and $AgNO_3$/PAN ratio (Figure S3). By controlling the viscosity of electrospinning solutions, the Ag/CNFs with different diameters in the range of ca. 30-500 nm can be obtained (Figure S4). In this work, the Ag/CNFs with diameter of 30 nm and 100 nm as typical samples are well investigated due to their smaller sizes resulting in better performance. Typically, the Ag/CNFs with diameter of 100 nm are produced by using PAN, $AgNO_3$ and glucose concentration of 4%, 2% and 1%, respectively, and heat treatment at 1000°C in NH_3 for 30 min with small flow rate. Figure 1 gives the SEM (a and b) and TEM (c and d) images of this Ag/CNF product. Clearly, the sample has continuously long fibrous morphology and uniform diameter. In comparison of Figure 1a with Figure S1a, much less heads of one-dimensional structures are found, indicating the higher L/D value of the Ag/CNFs. When comparing with the diameter of the as-spun nanofibers, that of the Ag/CNFs shrinks down from 200 nm to 100 nm after calcination due to polymer decomposition and NH_3-etching role. In addition, numerous silver nanoparticles with an average size of ca. 2

nm are observed, which uniformly distribute in the carbon fibers, and introducing them improves the conductivity of carbon nanofiber films from 167.2 Ω/sq to 57.2 Ω/sq.

The EDS spectrum shown in Figure 1b indicates that the hybrid nanofibers are mainly composed of C and Ag elements. Figure 1e and 1f show the XRD pattern and Raman spectrum of Ag/CNFs. The series of diffraction peaks at 2θ=38.1°, 44.3°, 64.5°, 77.5° and 81.5° can be assigned to the (111), (200), (220), (311) and (222) crystallographic planes of the face-centered cubic Ag (JCPDS No. 04–0783)[32]. And the broad peak around 22° obviously corresponds to (002) plan of graphite[33]. The Raman peaks at around 1360 cm^{-1} and 1585 cm^{-1} are attributed to the well-known D and G band, respectively.[34]

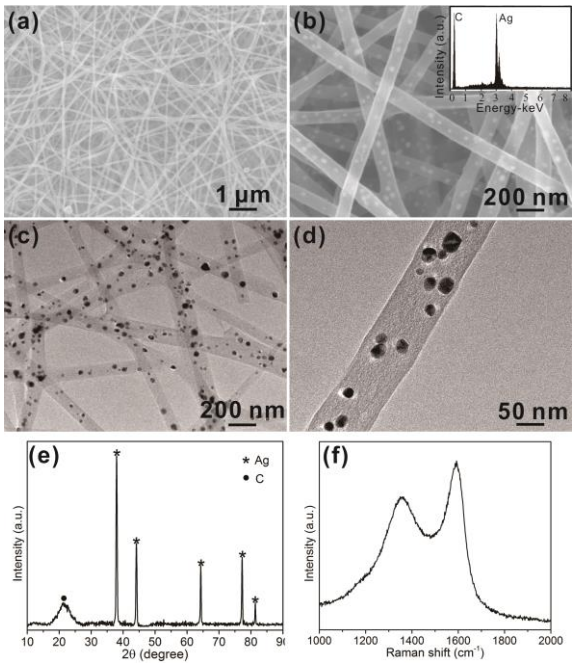

Figure 1 Characterizations of Ag/CNFs: (a) and (b) SEM images, (c) and (d) TEM images, (e) XRD pattern, and (f) Raman spectroscopy. And the inset in b is EDX spectrum.

The Ag/CNFs were used to fabricate transparent conductive films in the manner of partially substituting AgNWs. During the fabricating process, the filter membrane of mixed cellulose esters was turned into transparent film and simultaneously the adhesion of conductive materials on PET substrate was enhanced by adopting acetone vapor treatment.[35,36] Figure 2 provides the optical photos and corresponding SEM images of the hybrid films on PET substrates, as well as the transmittance and sheet resistance data. Obviously, the TCFs of pure AgNWs with surface concentration of 28 mg/m^2 possess good optical quality but poor conductivity due to incontinuous charge transfer network (Figure 2a). When the AgNWs concentration reaches 48 mg/m^2, the connection between AgNWs becomes good, leading to a relative low sheet resistance of ca. 132.7 Ω/sq (Figure 2b). Table S1 presents the relationship between deposition density of AgNWs and corresponding properties of conductivity and transmittance at 550 nm. On the other hand, the TCFs of pure Ag/CNFs with surface concentration of 120 mg/m^2 have poor conductivity either (Figure 2c). As we combine AgNWs with Ag/CNFs by simultaneously loading them with a concentration of 28 mg/m^2 and 120 mg/m^2, respectively, the obtained TCF sample has a transmittance of 75.6% and sheet resistance of 127.8 Ω/sq (Figure 2d). Such conductance is comparable to that of the TCFs prepared using pure AgNWs with a concentration of 48 mg/m^2, therefore the substitution of 41.7% for AgNWs was achieved if we can further improve the transmittance.

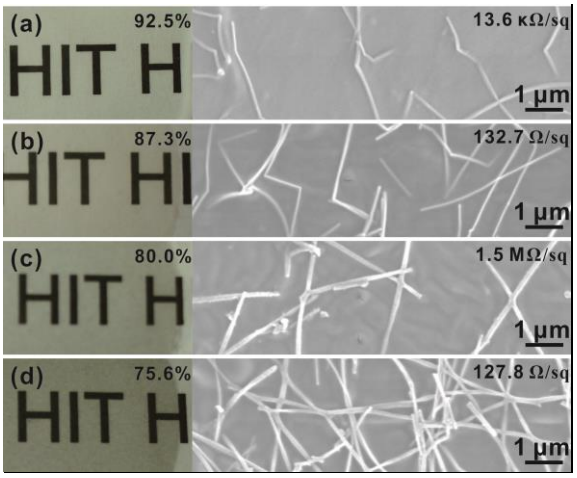

Figure 2 The left column exhibits digital photos of transparent films loaded with: (a) 28 mg/m^2 AgNWs; (b) 48 mg/m^2 AgNWs; (c) 120 mg/m^2 Ag/CNFs; (d) 28 mg/m^2 AgNWs and 120 mg/m^2 Ag/CNFs. The right column shows corresponding SEM images. And inset data present transmittance and sheet resistance, and the diameter of the used Ag/CNFs is 100 nm.

To increase the performance of the hybrid TCFs, the Ag/CNFs with different diameters from 30 nm to 500 nm were adopted. After fixing a sheet resistance of about 150 Ω/sq, the transmittance spectra of the TCFs producing by Ag/CNFs with different diameter were measured in the visible range from 380 nm to 800 nm. Despite of the strong light absorption of carbon component[37], the TCFs fabricated by Ag/CNFs with a diameter of 30 nm possess transmittance as high as about 88.0% at 550 nm wavelength (Figure 3a), attributed to the relatively large unoccupied space between conductive fibers (Figure 3b). With the increase of the fiber diameter from 100 nm to 500 nm, the transmittance decreased sharply because of stronger light absorption, scattering and reflection caused by bigger fiber diameter.[38] Therefore, the Ag/CNF composite fibers with smaller diameter are preferred for the fabrication of TCFs.

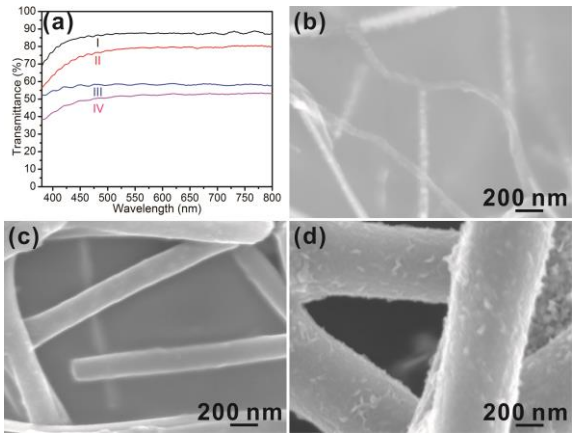

Figure 3 (a) Transmittance spectra of hybrid TCFs prepared using Ag/CNFs with different fiber diameter at same sheet resistance: I-diameter=30 nm, II-diameter=100 nm, III-diameter=200 nm, IV-diameter=500 nm. And SEM images of the distribution of Ag/CNFs with different diameters on hybrid TCF: (b) 30 nm; (c) 200 nm; (d) 500 nm.

The deposition order could made great effect on performance of the hybrid TCFs composed of Ag/CNFs and AgNWs, as shown in Figure S5. First decomposition of AgNWs can outspread on relative smooth surface, forming uniform conductive network and making full use of the excellent conductivity of AgNWs, thus giving a low sheet resistance of 135.9 Ω/sq. In the case of the other two deposition methods, the AgNWs deform more easily due to the flexibility of AgNWs and rough surface caused by Ag/CNFs, resulting in the difficulty to form uniform conductive connections.

Furthermore the influence of Ag/CNFs deposition density on the performance of the hybrid TCFs was investigated (Figure 4). It reveals that the sheet resistance increases slightly after decreasing to a valley value with the increase of deposition density of Ag/CNFs, and the valley value shifts towards higher deposition density of Ag/CNFs when decreasing the surface concentration of AgNWs. During the treatment in acetone vapour, the deposited Ag/CNFs enter into the substrate in company with the dissolution of the mixed cellulose esters, and this phenomenon would become more obvious when the treatment time gets longer. When further increasing the deposition density of Ag/CNFs, some of them are difficult to enter into the substrate due to its limited capacity, and thus they would appear on the surface of the TCFs, leading to the slight increase of the conductivity. And the thread shape of Ag/CNFs is also responsible for such tendency, with the similar principle to isotropical conductive adhesives (CIA) composed with CNT.[39] Additionally, as shown in Figure 4, the TCFs fabricated using Ag/CNFs with a diameter of 100 nm have the highest substitution value of about 41.7% at surface density of 28 mg/m^2 AgNWs, and the corresponding conductivity and transparency are 119.5 Ω/sq and 76.1%, respectively. As the fiber diameter decreases to about 30 nm, a result of 124.5 Ω/sq for conductivity and 88.0% for transparency could be achieved with the same substitution value. When the surface concentration of AgNWs increases to 38 mg/m^2, the highest substitution value shrinks down to 28.3% (Table S1), and in this case, the obtained TCFs possess the conductivity of 83.0 Ω/sq and transparency of 87.5%. And the increase of Ag/CNFs density results in the decrease of the transparency, so the balance between conductivity and transparency is very important for synthesizing TCFs with excellent performance.

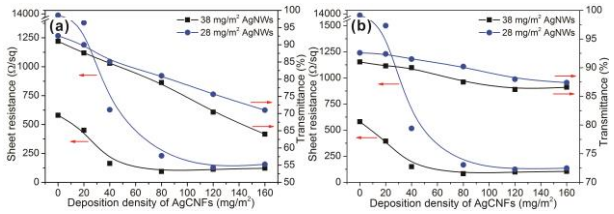

Figure 4 Variation of sheet resistance and transparency of hybrid TCFs as a function of deposition density of Ag/CNFs with two different fiber diameters: (a) 100 nm and (b) 30 nm. The lines with different shape and colour represent hybrid TCF fabricated at different AgNW surface density: the blue closed circle lines refer to 28 mg/m^2 and the dark closed square line refer to 38 mg/m^2.

The bending test of the AgNW-Ag/CNF hybrid TCFs is performed to investigate their flexibility (Figure 5a and b). From Figure 5a, negative angle bending leads to the increase of the sheet resistance less than 2% while the decrease of the sheet resistance less than 1% for positive angle bending. Figure 5b exhibits the variation in sheet resistance of a hybrid TCF as function of bending times after suffering the bending procedure from -180^o to 180^o. After 4000 times bending test, the sheet resistance of the TCF increases less than 4%. The adhesion of conductive fibers to the substrate was also tested by attaching a tape to the TCF and then peeling off. From Figure 5c, the sheet resistance of the TCF has no visible increase after repeated attaching and peeling cycles for 1000 times. The above results strongly suggest that the TCFs composed of AgNWs and Ag/CNFs possess excellent properties of flexibility and adhesion, which is favourable for flexible electronic devices.

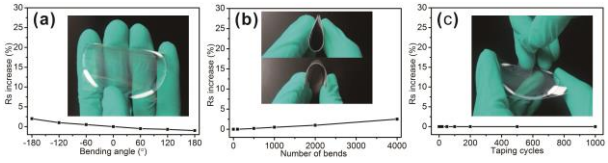

Figure 5 Mechanical property tests on flexible TCFs consisting of AgNWs and Ag/CNFs on PET substrates. (a) Sheet resistance versus bending radius. Inset is the photograph of bent hybrid TCF. (b) Sheet resistance versus bending number. Inset is the photograph of the bending procedure. (c) Sheet resistance versus cycle numbers of taping and peeling. Inset is the photograph of the taping procedure.

To evaluate the thermal stability of the TCFs composed of different conductive materials, they were kept in furnace for 2 hours at different temperatures. Figure 6a shows the changes of the sheet resistance during the thermal oxidation test. The sheet resistance of the AgNW-based TCF drastically increases more than 5000% when treated at 155°C. Such rapid increase of resistance is probably attributed to partial destruction of conductive AgNW network caused by heat-induced welding of adjacent AgNWs. However the sheet resistance of the pure Ag/CNF-based TCF increases no more than 20% after experiencing same heat treatment due to the good resistance of carbon element to high temperature. The similar reason can be used to explain the phenomenon of the slow increase of sheet resistance in the hybrid TCF composed of AgNWs and Ag/CNFs. When treated at higher temperatures, the resistance gradually reaches a certain constant value, which is determined by the amount of Ag/CNFs. Interestingly, the resistance of the TCFs decreases at relatively low temperature and reaches a minimum value at about 130°C (inset of Figure 6a). The enhancement of the conductivity probably lies in the melting behaviour between AgNW-AgNW and AgNW-Ag/CNF at cross section (Figure S6a and b).

Furthermore, the stability of the TCFs in the corrosive environment of HCl solution was probed into (Figure 6b). The sheet resistance of the AgNW-based TCF increases much faster than that of the AgNW and Ag/CNF-based TCF, however the resistance of the Ag/CNF-based TCF has no obvious change. Besides, high concentration of HCl solution could accelerate the corrosion process of AgNWs, leading to great increase of sheet resistance. Slight improvement of conductivity can also be detected at the beginning of acid treatment and a minimum value is reached at about 10 minutes. It is deduced that the enhanced conductivity is caused by removing the surface oxide layer of AgNWs, and that the collapse of conductive network resulting in significant increase of resistance results from the corrosion of vast amount of AgNWs, which is clearly observed in Figure S6d. Since proper heat and acid treatment can increase the conductivity of TCFs, the hybrid TCFs were immersed into HCl solution for 10 min and then heated at 130°C for 2 h. The sheet resistance of hybrid TCF can be further improved from 83.0 Ω/sq to 50.0 Ω/sq with almost no changes in the transmittance.

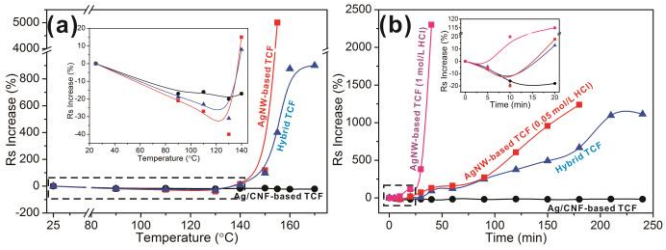

Figure 6 Stability tests in different environment: (a) thermal oxidation and (b) HCl acid corrosion. Insets magnify the area of dotted line. And all the selected TCFs have similar sheet resistance.

In order to demonstrate the potential suitability of the hybrid TCFs consisting of AgNWs and Ag/CNFs for optoelectronic devices, we fabricated two electrical lines through masking the substrate, and then the positive and negative electrodes of LED lamps were connected with the lines to form a simple device (Figure 7). As the LED lamps were powered on, they were lightened thoroughly. From the photograph, it can be confirmed that the device is highly transparent and flexible. Therefore, the hybrid TCFs developed here hold high promise in many flexible optoelectronic devices

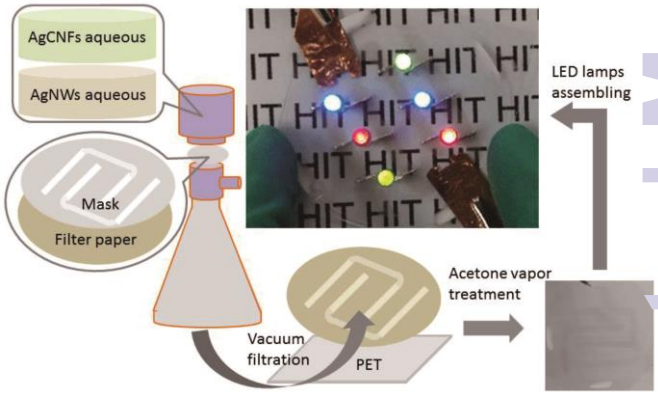

Figure 7 Manufacturing procedures of patterned TCF and its use in LED lamp arrays.

4. Conclusions

In summary, we developed a simple and inexpensive method to produce highly conductive flexible films with excellent optical transparency, which was realized through partially substituting AgNWs by electrospinning-derived Ag/CNFs. The silver nanoparticles were introduced and uniformly distributed in the carbon nanofibers, which improve the conductivity of the carbon nanofibers and provide active sites to promote the combination of AgNWs and Ag/CNFs, decreasing the contact resistance between the conductive materials and thus further enhancing the conductivity of TCFs significantly. Moreover, the fiber diameter exerted great effects on the performance of the TCFs, and the hybrid TCFs based on AgNWs and Ag/CNFs with a diameter of ca. 30 nm exhibited excellent properties of a sheet resistance of 50.0 Ω/sq and transmittance of 87.5% because of the large unoccupied spaces induced by smaller fiber diameter. Besides, the Ag/CNF-based TCFs showed high flexibility during bending test and stability to harsh environments of thermal oxidation and HCl acid corrosion due to the good stability of carbon element. Therefore, the TCFs developed here are a highly promising candidate for the applications in flexible transparent conductive devices.

Acknowledgements

The work was financially supported by NSFC 51102064 and Shenzhen Bureau of Science, Technology and Innovation Commission (JCYJ20120613134244467 and JCYJ20140417172417151).

Notes and references

1. K. A. Sierros, N. J. Morris, K. Ramjiand D. R. Cairns, *Thin solid films*, 2009, **517**, 2590.
2. D. R. Cairns, R. P. Witte II, D. K. Sparacin, S. M. Sachsman, D. C. Paine and G. P. Crawford, *Appl. Phys. Lett.*, 2000, **76**, 1425.
3. P. A. Levermore, R. Jin, X. Wang, L. Chen, D. D. C. Bradley and J. C. D. Mello, *J. Mater. Chem.*, 2008, **1837**, 4414.
4. D. Alemu, H. Y. Wei, K. C. Ho and C. W. Chu, *Energ. Environ. Sci.*, 2012, **5**, 9662.
5. S. I. Na, S. S. Kim, J. Jo and D. Y. Kim, *Adv. Mater.*, 2008, **20**, 4061.
6. L. Hu, D. S. Hecht and G. Grüner, *Nano Letters*, 2004, **4**, 2513.
7. M. F. Mabrook, C. Pearson, A. S. Jombert, D. A. Zeze and M. C. Petty, *Carbon*, 2009, **47**, 752.
8. M. W. Rowell, M. A. Topinka, M. D. Mcgehee, H. J. Prall, G. Dennler and N. S. Sariciftci, *Appl. Phys. Lett.*, 2006, **88**, 233506.
9. A. K. Geim, *Nat. Mater.*, 2007, **6**, 183.
10. G. Eda and M. Chhowalla, *Adv. Mater.*, 2010, **22**, 2392.
11. P. H. Wobkenberg, G. Eda, D. Leem, J. C. De Mello, D. D. C. Bradley, M. Chhowalla and T. H. Anthopoulos, *Adv. Mater.*, 2011, **23**, 1558.
12. D. Reibold, F. Shao, A. Erdmann and U. Peschel, *Opt. Express*, 2009, **17**, 544.
13. M. Kang, M. Kim, J. Kim and L. J. Guo, *Adv. Mater.*, 2008, **20**, 4408.
14. C. Bao, J. Yang, H. Gao, F. Li, Y. Yao, B. Yang and Z. Zou, *ACS Nano*, 2015, **9**, 2502.
15. X. Y. Zeng, Q. K. Zhang, R. M. Yu and C. Z. Lu, *Adv. Mater.*, 2010, **22**, 4484.
16. D. S. Leem, A. Edwards, M. Faist, J. Nelson, D. D. C. B. And and J. C. D. Mello, *Adv. Mater.*, 2011, **23**, 4371.
17. T. Kim, A. Canlier, G. H. Kim, J. Choi, M. Park and S. M. Han, *ACS Appl. Mater. Interfaces*, 2012, **5**, 788.
18. T. L. Chen, D. S. Ghosh, V. Mkhitaryan and V. Pruneri, ACS *Appl. Mater. Interfaces*, 2013, **5**, 11756.
19. J. H. Lee, H. S. Shin, Y. J. Noh, S. I. Na and H. K. Kim, Sol. *Energ. Mat. Sol. C.*, 2013, **114**, 15.
20. C. Mayousse, C. Celle, A. Carella and J. P. Simonato, *Nano Res.*, 2014, **7**, 315.
21. A. Kumar and C. Zhou, *ACS Nano*, 2010, **4**, 11.
22. L. Hu, S. K. Han, J. Y. Lee, P. Peumans and C. Yi, *ACS Nano*, 2010, **4**, 2955.
23. C. H. Liu and X. Yu, *Nanoscale Res. Lett.*, 2011, **6**, 75.
24. J. L. Elechiguerra, L. Larios-Lopez, C. Liu, D. Garcia-Gutierrez, A. Camacho-Bragado and M. J. Yacaman, *J. Chem. Mate* 2005, **17**, 6042.
25. Z. Wang, J. Liu, X. Chen, J. Wan and Y. Qian, *Chem-Eur. J.*, 2005, **11**, 160.
26. E. C. Garnett, W. Cai, J. J. Cha, F. Mahmood, S. T. Connor, M G. Christoforo and M. L. Brongersma, *Nat. Mate.*, 2012, **11**, 241.
27. S. De, T. M. Higgins, P. E. Lyons, E. M. Doherty, P. N. Nirmalraj, W. J. Blau and J. N. Coleman, *ACS Nano*, 2009, **3**, 1767.
28. T. Tokuno, M. Nogi, M. Karakawa, J. Jiu, T. T. Nge, Y. Aso and K. Suganuma, *Nano Res.*, 2011, **4**, 1215.
29. H. W. Tien, S. T. Hsiao, W. H. Liao, Y. H. Yu, F. C. Lin, Y. S. Wang, S. M. Li and C. C. M. Ma, *Carbon*, 2013, **58**, 198.
30. X. Zhang, X. Yan, J. Chen and J. Zhao, *Carbon*, 2014, **69**, 43
31. A. J. Stapleton, R. A. Afre, A. V. Ellis, J. G. Shapter, G. G Andersson, J. S. Quinton and D. A. Lewis, *Sci. Technol. Adv. Mat.*, 2013, **14**, 35004.
32. J. Q. Hu, Q. Chen, Z. X. Xie, G. B. Han, R. H. Wang, B. Ren and Z. Q. Tian, *Adv. Funct. Mater.*, 2004, **14**, 183.
33. Z. Wang, H. Wang, B. Liu, W. Qiu, J. Zhang, S. Ran and G. Shen, *ACS Nano*, 2011, **5**, 8412.
34. K. Blinn, H. Abernathy, X. Li, M. Liu, L. A. Bottomley, M. Liu, *Energ. Environ. Sci.*, 2012, **5**, 7913.
35. J. S. Webber, A. G. Czuhanich and L. J. Carhart, J. *Occup. Environ. Hyg.*, 2007, **4**, 780.
36. Z. Wu, Z. Chen, X. Du, J. M. Logan, J. Sippel, M. Nikolou and A. G. Rinzler, *Science*, 2004, **305**, 1273.
37. Y. Zhou, L. Hu and G. Gruner, *Appl. Phys. Lett.*, 2006, **88**, 123109.
38. Y. C. Lu and K. S. Chou, *Nanotechnology*, 2010, **21**, 215707.
39. H. P. Wu, X. J. Wu, M. Y. Ge, G. Q. Zhang, Y. W. Wang, J. Jiang, *Compos. Sci. Technol.*, 2007, **67**, 1182.